

Degradation of the Transmissive Optics for a Laser-Driven IFE Power Plant under Electron and X-Ray Irradiation^{*)}

Vladimir D. ZVORYKIN, Andrei S. ALIMOV¹⁾, Sergei V. ARLANTSEV²⁾,
Boris S. ISHKHANOV¹⁾, Alexei O. LEVCHENKO, Nikolai N. MOGILENETZ³⁾,
Victor F. ORESHKIN, Andrei P. SERGEEV, Pavel B. SERGEEV, Victor F. SHTAN'KO⁴⁾,
Vasilii I. SHVEDUNOV¹⁾ and Nikolai N. USTINOVSKII

P.N. Lebedev Physical Institute of RAS, Leninsky Prospect 53, Moscow, 119991, Russia

¹⁾*D.V. Skobel'tsyn Institute of Nuclear Physics, Moscow State University, Vorob'evy gory 1, Moscow, 119992, Russia*

²⁾*V.K. Orlov OKB "Granat", Volokolamskoe Shosse 95, Moscow, 125424, Russia*

³⁾*National Research Nuclear University "MEPhI", Kashirskoe Shosse 31, Moscow, 115409, Russia*

⁴⁾*Tomsk Polytechnic University, Tomsk, Prospect Lenina 30, 634050, Russia*

(Received 1 June 2012 / Accepted 31 July 2012)

Several facilities are used to test transmissive optics of the IFE target chamber and KrF laser driver in regard of transient and residual radiation-induced absorption in the range of 150–1200 nm. Comparative study of radiation darkening of various fused silica glasses, high-purity CaF₂, MgF₂, and Al₂O₃ crystals under irradiation by 300-keV electrons, soft ($h\nu = 6\text{--}20\text{ keV}$) and hard ($h\nu \sim 400\text{ keV}$) X-rays is done and better radiation-proof optical materials are selected; the opposite effect of optics bleaching under UV laser light is observed.

© 2013 The Japan Society of Plasma Science and Nuclear Fusion Research

Keywords: darkening of fused silica glasses and UV crystals under irradiation by fast electrons, soft and hard X-rays

DOI: 10.1585/pfr.8.3405046

1. Introduction

While Thermo Nuclear (TN) ignition experiments are underway at the LLNL, USA aiming at demonstration of a feasibility of the general concept to produce Inertial Fusion Energy (IFE) with laser drivers, a huge scientific and technological work is ahead to realize the first laser-driven power-production plant. Only 3ω (or 2ω) Diode Pumped Solid State Laser (DPSSL) and e-beam-pumped Krypton Fluoride (KrF) laser can operate for a long time at a repetition rate of 5–10 Hz with high pulse energy $\sim 1\text{ MJ}$ and overall efficiency $\sim 7\%$ to satisfy the requirements for the future IFE power plant [1, 2].

Large-size, high laser strength and radiation resistant optics, which collects numerous laser beams and directs them onto TN capsule is one of the critical issues for the IFE reactor. The highest radiation load falls to so-called final optics. Being in the line of sight with an exploding TN target it assumes direct impact of target release products, i.e. neutrons, γ -rays, X-rays, ions, and target debris. In different IFE layouts of LIFE (LLNL, USA), FTF (NRL, USA) and KOYO-F reactors (ILE, Japan) thin ($\sim 5\text{ mm}$) fused silica Fresnel lenses [3] or grazing incidence metal mirrors [4] (or even liquid metal mirrors [5]) are projected to deflect incoming laser beams towards a target. Nevertheless, scattered radiation can affect on the other optical

elements, i.e. windows of a reactor chamber, turning mirrors etc.

Another problem to be solved is a degradation of the internal optics of large-scale KrF laser drivers, pumped by relativistic e-beams. Laser windows are irradiated by scattered fast electrons (indeed, they can be highly reduced in a guiding magnetic field), intense UV laser light, and bremsstrahlung X-rays produced by e-beam deceleration when being transported from vacuum diodes into a laser chamber and pumping a working gas [6, 7]. X-ray dose absorbed in KrF laser windows expected for a 1-year duty IFE reactor cycle might cause a strong degradation of their transmittance. Darkening of initially transparent optical materials (OM) is caused by knock-on of atoms from a lattice by neutrons or by initial point structural defects, both of which trap radiation-produced electrons and holes with creating color centers [8–10].

We describe test-bench facilities for comparative studies of various OM suitable for transmissive optics or coatings at wavelengths of KrF and 3ω (2ω) DPSSL. Fused silica glasses of Corning 7980, Russian KU-1 and KS-4V, crystals CaF₂, MgF₂, and Al₂O₃ were tested in regard of short-lived (transient) and long-lived (residual) absorption induced in the spectral range of 150–1200 nm by 300-keV electrons, soft ($h\nu = 6\text{--}20\text{ keV}$) and hard ($h\nu \sim 400\text{ keV}$) X-rays.

author's e-mail: zvorykin@sci.lebedev.ru

^{*)} This article is based on the presentation at the Conference on Inertial Fusion Energy '12.

2. GARPUN KrF Laser

2.1 Characterization of bremsstrahlung X-ray emission

GARPUN KrF laser [11] designed for amplification of subpicosecond to nanosecond UV pulses is a well-characterized test-bench facility regarding to Bremsstrahlung X-ray yield [7]. The main amplifier of this facility (Fig. 1) has a gas chamber with dimensions $19 \times 22 \times 140$ cm, and it is pumped by two counter-propagating e-beams of the area 12×100 cm² guided by ~ 0.1 -T pulsed magnetic field, which provide specific pumping power up to 0.8 MW/cm³. E-beams with 60-kA total current, electron energy of $\varepsilon_e \sim 300$ keV, and 75-ns pulse duration (FWHM) are accelerated in vacuum diodes and coupled into the gas chamber laterally to the laser axis through vacuum-tight 20- μ m thickness Ti foils with stainless steel support.

Bremsstrahlung spectrum was reconstructed from time-resolved scintillation measurements of X-ray absorption in Al, Cu and Pb plates of different thickness (Fig. 2) by using the developed regularization algorithm for solving an integral equation [7].

The maximum of reconstructed X-ray spectrum lies in the range of photon energies $h\nu = 70$ – 100 keV (Fig. 3).

X-ray fluence onto laser windows was measured by

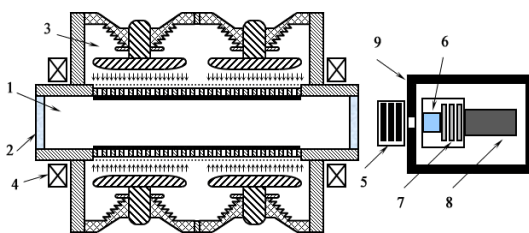


Fig. 1 Layout of GARPUN main amplifier equipped for X-ray measurements – (1) gas chamber; (2) window; (3) vacuum diode; (4) solenoid; (5) X-ray absorbers; (6) NaI scintillator; (7) neutral filters; (8) photomultiplier; (9) X-ray shielding.

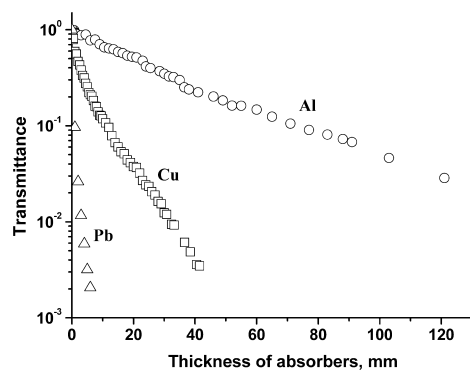


Fig. 2 Attenuation of X-ray radiation in Cu, Al, and Pb absorbers of different thickness.

calibrated 1-mm-thick Al₂O₃ TLD detectors being set in a stack inside the laser chamber nearby the window. Energy fluence was found to be $F_{X\text{-ray}} \sim 10^{-3}$ J/cm² per e-beam shot for typical gas pressure of 1.4 atm in the chamber and a half of this value for evacuated chamber.

Using the obtain data one can estimate X-ray fluence $F_{X\text{-ray}} \sim 10^{-2}$ J/cm² in a single shot which is expected at the window of 100-kJ ICF-scale KrF amplifier with a gain volume of $2 \cdot 10^6$ cm³, specific pumping power 0.4 MW/cm³, e-beam energy $\varepsilon_e = 600$ keV, and pulse duration 600 ns [2, 6, 12]. That corresponds to total absorbed dose accumulated over $N = 10^8$ shots (for a 1-year operation) $D = N(\mu_a/\rho) F_{X\text{-ray}} \sim 30$ MGy, where the ratio of mass absorption coefficient to density $\mu_a/\rho \sim 0.03$ cm²/g for various OM and X-ray quanta energy $\varepsilon_{X\text{-ray}} = 10^2$ – 10^3 keV.

2.2 X-ray induced transient absorption

Transient X-ray induced absorption during X-ray pulse was measured at Berdysk preamplifier of GARPUN KrF laser facility [13]. Its gain volume is approximately one quarter of the main GARPUN amplifier, and it is one-side pumped by e-beam of 8×110 cm² area, with the same electron energy $\varepsilon_e = 300$ keV and 75-ns pulse duration. Thus, X-ray fluence onto the preamplifier windows is one quarter of the bigger amplifier.

Transient X-ray-induced absorption was measured in a multi-pass layout with probe pulsed radiation of KrF ($\lambda = 248$ nm) or coumarin-47 dye laser ($\lambda = 460$ nm) [14] in evacuated laser chamber to eliminate absorption in the gas (Fig. 4).

For a uniform distribution of absorbed X-ray doses in the windows (which is just the case of the large X-ray range compared with window thickness) transient induced absorption coefficients were found $\alpha_{tr} \approx 0.015$ cm⁻¹ in CaF₂ and $\alpha_{tr} \approx 0.01$ cm⁻¹ in SiO₂, approximately equal at both wavelengths. Being rather small in current experiments at low X-ray fluence $F_{X\text{-ray}} \sim 10^{-4}$ J/cm², transient absorption may be significant under the IFE-scale conditions with expected $F_{X\text{-ray}} \sim 10^{-2}$ J/cm².

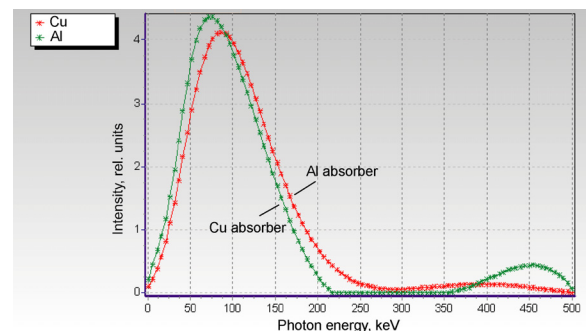


Fig. 3 Bremsstrahlung X-ray spectra obtained at processing of Cu and Al absorption curves.

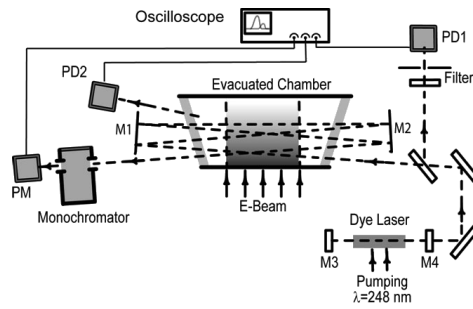


Fig. 4 A multi-pass layout for transient X-ray-induced absorption measurements.

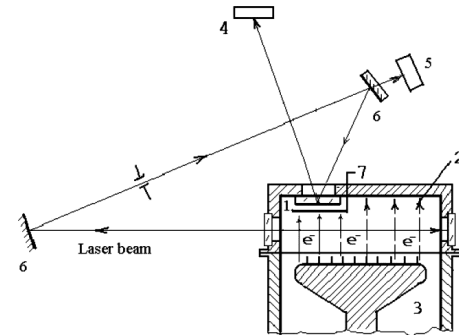


Fig. 5 Layout of e-beam-induced transient absorption measurement at EL-1 excimer laser – (1) tested sample; (2) e-beam; (3) vacuum diode; (4, 5) calorimeters; (6) mirrors; (7) shutter.

3. E-Beam-Pumped EL-1 Excimer Laser

Although in properly designed KrF laser an escape of scattered e-beam electrons has a small effect on the windows [13], pulsed e-beam gun of EL-1 facility (280-keV, 200-A/cm², 80-ns) was shown to be a convenient tool in studying of structural defects formation and relaxation [15–17]. Up to 15,000 e-beam shots have been done to irradiate OM samples with energy fluence of $F_e \sim 2 \text{ J/cm}^2$. In contrast to X-rays, e-beam is absorbed in a thin surface layer of $\sim 100\text{-}\mu\text{m}$ thickness which gives very high local absorbed doses of $\sim 50 \text{ kGy}$ per shot.

3.1 Transient absorption

Transient absorption in the OM during e-beam irradiation was measured (Fig. 5) at different operation wavelengths of the EL-1 excimer laser with ArF ($\lambda = 193 \text{ nm}$), KrF ($\lambda = 248 \text{ nm}$) and XeF ($\lambda = 353 \text{ nm}$). The ratio of calorimeters readings was measured with a shutter (7) closed and open. From these measurements an optical density (*OD*) of e-beam-induced transient absorption at the laser wavelength was found, being proportional to e-beam power density $OD = K \cdot F_e / \tau$ where pulse duration $\tau = 80 \text{ ns}$. Coefficients of proportionality *K* for different SiO₂ and CaF₂ samples are given in Table 1.

Table 1 Measured *K* [cm²/GW] for different OM samples at wavelengths of 193, 248 and 353 nm.

OM	353 nm	248 nm	193 nm
KS-4V	1	4	6
Corning-ArF	0.6	1.1	0.6
Corning-KrF	0.9	1.7	8
Corning-stand	1	2.7	6
KU-1	0.6	2	4
CaF ₂	53	50	72

3.2 Residual absorption

Figure 6 demonstrates a typical *OD* spectrum (1) of ArF-grade Corning 7980 glass after a successive e-beam irradiation in 3250 shots with a cumulative energy fluence of $F_{e\Sigma} \sim 6.5 \text{ kJ/cm}^2$ [17]. When being decomposed into individual absorption bands it contains the most intensive bands centered at 163 (2) and 245 nm (6) belonging to the oxygen-deficient centers (ODC); at 213 nm (4) – E' centers arising from the ODC by losing an electron; at 183 (3) and 260 nm (7) – non-bridging oxygen hole centers (NBOHC). A band (5) which is observed at 225 nm is not interpreted yet. The intensity of the ODC band at 245 nm is rather low compared with combined neutron and γ -ray irradiation [8, 9]. It is seen that the most of residual induced absorption arises in the VUV and UV spectral ranges while

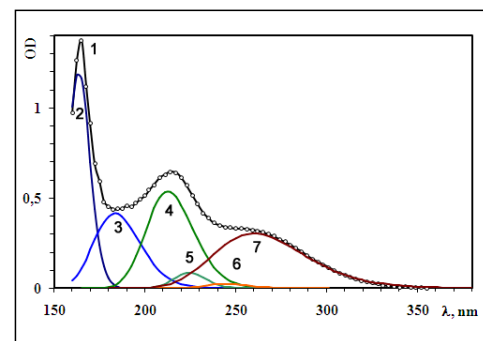


Fig. 6 E-beam induced *OD* spectrum of ArF-grade Corning 7980 glass and its constituent bands.

for wavelengths $\lambda > 350 \text{ nm}$ it is rather small.

Although e-beam induced *OD* spectra for the other SiO₂ glasses under testing were qualitatively similar, significant variation was observed in contribution of different individual absorption bands.

The dependences of maximal e-beam induced *OD* in individual absorption bands on cumulative energy fluence for KS-4V and KU-1 glasses are compared in Figs. 7, 8. At $F_{e\Sigma} = 4\text{--}5 \text{ kJ/cm}^2$ absorption in all bands tends to saturation at rather different level for various OM.

Minimal saturated absorption in the UV range around KrF laser wavelength was observed for KS-4V glass,

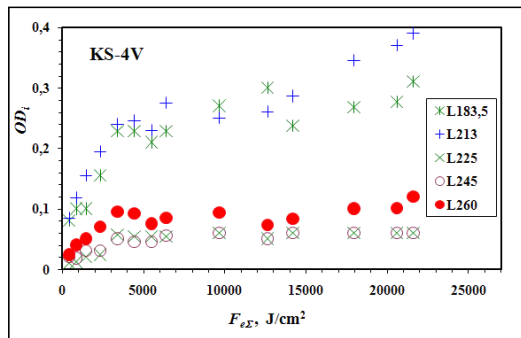


Fig. 7 Maximal e-beam induced OD in individual absorption bands vs. cumulative energy fluence for KS-4V glass.

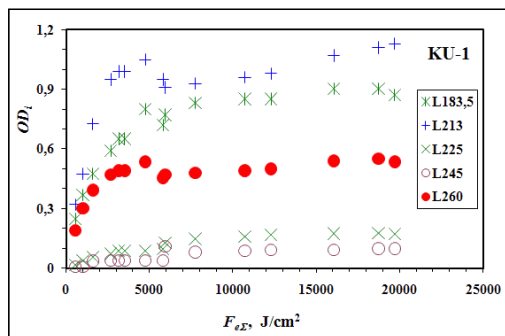


Fig. 8 Maximal e-beam induced OD in individual absorption bands vs. cumulative energy fluence for KU-1 glass.

which has very low content of hydroxyl – less than 0.1 ppm and of chlorine less than 20 ppm. Compared with this “dry” glass hydroxyl concentration in “wet” glasses Corning 7980 and KU-1 amounts to approximately 1000 ppm, while other impurities (mainly chlorine) varies from ~200 ppm in KU-1 to 20 ppm in ArF-grade Corning 7980 glass. Note, that KS-4V glass demonstrated better stability against neutron and γ -ray irradiations also [10].

Among other OM the best stability against e-beam irradiation demonstrates Al_2O_3 . In contrast to neutrons and γ -ray irradiation [10] its transmittance did not change at all after $F_{e\Sigma} \sim 30 \text{ kJ/cm}^2$. Transmittance of CaF_2 around $\lambda = 248 \text{ nm}$ for the same irradiation fell down by 5–10%. Oppositely, MgF_2 demonstrated very high degradation.

3.3 Bleaching effect of UV laser radiation upon e-beam-irradiated optical samples

Windows of e-beam-pumped KrF lasers are exposed to a variety of ionizing radiations including UV laser light. The behavior of SiO_2 glasses subjected to such complex action were performed with tested samples mounted at the place of laser window being irradiated by scattered e-beam electrons with the fluence $F_e \sim 0.4 \text{ J/cm}^2$ and by laser fluence $F_{L1} \sim 0.35 \text{ J/cm}^2$ per pulse (corresponding to $\sim 4.4 \text{ MW/cm}^2$ intensity in 80-ns laser pulse) [16]. To make

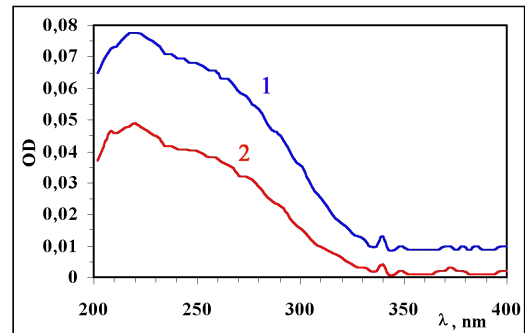


Fig. 9 Induced OD spectra of ArF-grade Corning 7980 glass exposed to e-beam only (1) and simultaneously to e-beam and KrF laser light (2).

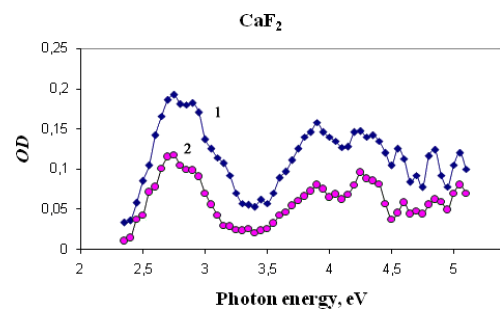


Fig. 10 E-beam-induced OD spectrum in CaF_2 at 10 (1) and 500 ns (2) after the e-beam pulse with $F_e = 0.1 \text{ J/cm}^2$.

a control measurement one half of the sample surface was shadowed against laser light being exposed only to e-beam. Figure 9 shows typical induced absorption OD spectra of ArF-grade Corning 7980 sample after 400 shots of exposing to the e-beam only and after simultaneous exposing to the e-beam and laser radiation. Higher transmission is observed for the simultaneous irradiation. It is a result of two opposite processes of the glass darkening due to color centers formation under e-beam and their mutual relaxation hastened by UV light. For various SiO_2 glasses induced OD at $\lambda = 248 \text{ nm}$ in the case of dual irradiation was about 1.5 times less.

4. E-Beam Induced Time-Resolved Absorption Spectra

Time-resolved pulsed spectroscopy in the range of $\lambda = 200\text{--}1100 \text{ nm}$ was used to measure with 7-ns resolution relaxation of transient absorption centers produced in OM by a short e-beam pulse (280-keV, 0.5 J/cm^2 , 12 ns). Transient absorption in SiO_2 glasses and CaF_2 being measured with different time delays after e-beam pulse was a superposition of many individual absorption bands.. Absorption in these bands belonging to different short-lived centers exponentially decays in CaF_2 with different characteristic times of 0.4 to 1.7 μs (Fig. 10).

The time behavior of e-beam induced OD relaxation

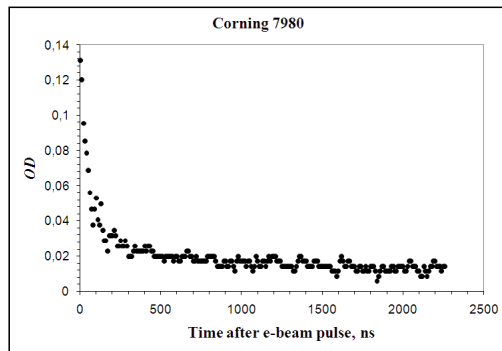


Fig. 11 Time relaxation of induced absorption OD in Corning 7980 glass at $\lambda = 320$ nm.

in Corning 7980 glass at $\lambda = 320$ nm at the initial stage is close to a hyperbolic law while at longer times a long-lived absorption reveals itself (Fig. 11).

5. LINAC-Based Hard X-Ray Source

5.1 Characterization of the source

A bremsstrahlung hard X-ray source was developed on the basis of a quasi-CW electron LINAC with maximum e-beam energy of 1.2 MeV and e-beam power of 60 kW [18]. A layout of the accelerator (Fig. 12 left) includes an electron gun (1) placed at the input of the first accelerating section (4), a second accelerating section (5), two klystrons with a maximum output power of 50 kW (2, 3), supplying wave guides (6, 7) with ports for vacuum pumping (8, 9). The beam ejection system includes a vertical (transverse) scanning magnet (11), a horizontal (longitudinal) scanning magnet (12), and a chamber for e-beam ejection into the atmosphere (13). After the first accelerating section, the e-beam has energy of 600 keV, after the second section, at the accelerator output, the energy is 1.2 MeV. The average e-beam current varies in the range from 0 to 50 mA. A 600-keV regime was chosen in present experiments as it is close to typical e-beam energy of the IFE-scale KrF laser driver.

For bremsstrahlung production Ta target of 0.3-mm thick, cooled by water (Fig. 12 right) was mounted at the exit of the first accelerating section in position (10). Irradiated OM samples were placed at 0.55 to 5.9 cm distances from the bremsstrahlung target. Absorbed doses of X-ray radiation were measured by calibrated nickel-activated SiO_2 glass dosimeters DTS-0.01/1, which were placed directly in the location of irradiated samples. X-ray dose rate 30 Gy/s was measured at the minimal 0.55-cm distance from the bremsstrahlung target within the area 2.5 cm at e-beam current ~ 5 mA, for which steady accelerator performance was maintained for dozen of hours. Thus, absorbed X-ray doses in tested samples in excess of 1 MGy were available. To evaluate the X-ray spectrum Pb absorbers were used and the dependence of the dose obtained by

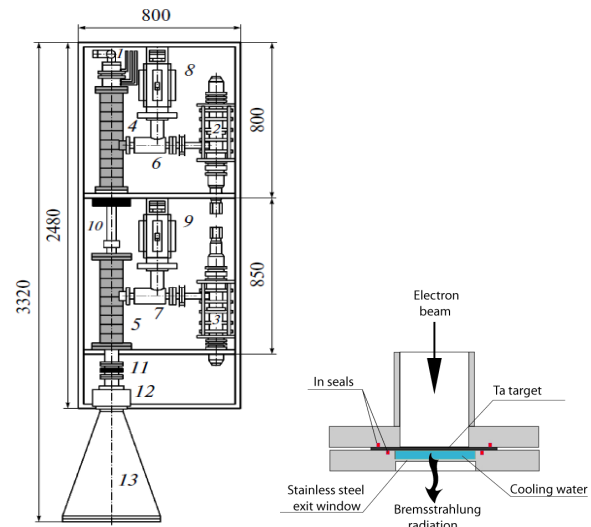


Fig. 12 Layout of the LINAC (left) and bremsstrahlung x-ray converter (right).

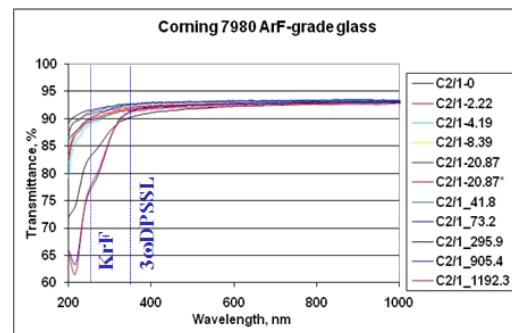


Fig. 13 Transmittance spectra of ArF-grade Corning 7980 glass before and after irradiation by hard x-rays with different absorbed doses (shown in the insert in kGy).

DTSs on absorber thickness was measured. The average energy of bremsstrahlung quanta $h\nu \approx 400$ keV was found, the maximum energy being $h\nu \approx 600$ keV.

5.2 Residual X-ray induced absorption

Transmission spectra of Ar-grade Corning 7980 and KS-4V glasses before and after successive runs of X-ray irradiations with increasing absorbed doses (their values in kGy are shown in the inserts) are compared in Figs. 13, 14. Once again “dry” KS-4V glass demonstrates better radiation stability in the UV range than Ar-grade Corning 7980, the best among “wet” glasses.

For volumetric X-ray absorption in the samples residual induced absorption coefficient α was found at KrF laser wavelength for different OM. All samples demonstrated gradual increase of α in dependence on cumulative absorbed X-ray dose although sometimes not monotonous (Fig. 15). A tendency to saturation was also observed; the saturated values at $\lambda = 248$ nm were the least for

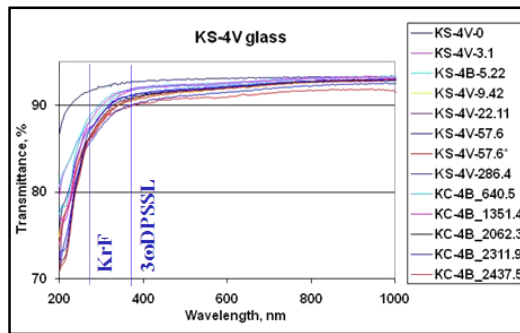


Fig. 14 Transmittance spectra of KS-4V glass before and after irradiation by hard x-rays with different absorbed doses (shown in the insert in kGy).

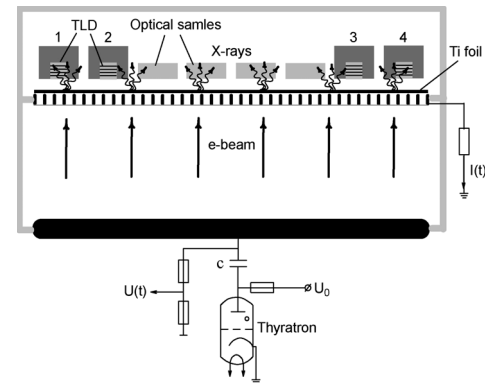


Fig. 16 Layout of rep-rate glow-discharge soft x-ray source.

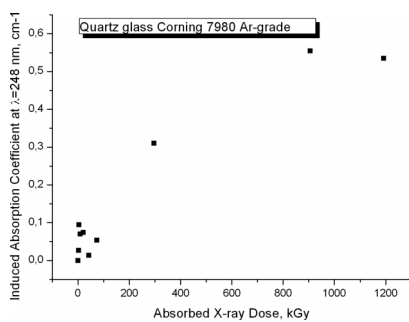


Fig. 15 Residual induced absorption coefficient at $\lambda = 248$ nm vs. cumulative absorbed X-ray dose in Ar-grade Corning 7980 glass.

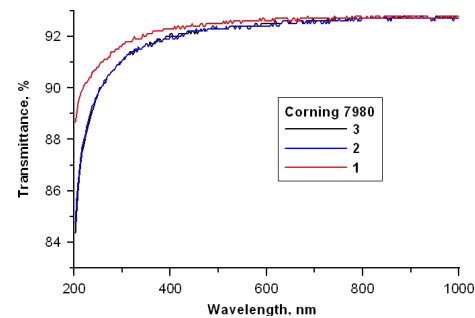


Fig. 17 Transmittance of two Corning 7980 samples before (1) and after (2, 3) soft X-ray irradiation with cumulative fluence $F_{X\text{-ray}} = 7.9 \text{ J/cm}^2$.

Al_2O_3 ($\alpha_{\text{sat}} = 0.025\text{--}0.030 \text{ cm}^{-1}$) and CaF_2 ($\alpha_{\text{sat}} = 0.11\text{--}0.12 \text{ cm}^{-1}$), while among the glasses KS-4V was the best ($\alpha_{\text{sat}} = 0.21\text{--}0.25 \text{ cm}^{-1}$). Note that for a rep-rate KrF laser driver operation inter shot self annealing could be expected.

6. Glow Discharge Soft X-Ray Source

Rep-rate X-ray source based on high-voltage glow discharge (Fig. 16) produced average radiation intensity 2–3 mW/cm^2 in a 50-Hz train of $\sim 1\text{-}\mu\text{s}$ pulses with photon energy of $h\nu = 6\text{--}20 \text{ keV}$ [19].

Being absorbed in a thin surface layer of 0.1–1 mm soft X-rays produce dose rates up to 5 Gy/s. Just in this range there is the most of plasma X-ray release of an imploding TN target. Also, at $h\nu \sim 2 \text{ keV}$ characteristic K lines of Ar and Kr (contained in a working gas mixture) give significant contribution into X-ray spectrum illuminating KrF laser driver windows. The response of Corning 7980 glass to soft X-ray radiation (Fig. 17) was something stronger if compared with e-beam irradiation.

7. Summary

Short-lived and long-lived absorption induced by 300-keV electrons and X-rays in optical materials were mea-

sured at the single-shot e-beam-pumped KrF GARPUN and excimer EL-1 lasers. Various glasses Corning 7980, KU-1, KS-4V, and crystals CaF_2 , MgF_2 , Al_2O_3 were tested to find the most stable for the IFE optics. Optics response to hard X-ray photons ($h\nu \sim 400 \text{ keV}$) was studied at a linac-based powerful quasi-CW source with a dose rate $\sim 30 \text{ Gy/s}$ and total amassed doses as high as 1–2 MGy. A rep-rate soft X-ray source ($h\nu = 6\text{--}20 \text{ keV}$, 1- μs , 50-Hz) on the base of high-voltage glow discharge produced dose rate $\sim 5 \text{ Gy/s}$ in a thin surface layer. All types of ionizing radiation caused optics darkening especially at KrF laser wavelength.

[1] I.N. Sviatoslavsky, M.E. Sawan, R.R. Peterson *et al.*, Fusion Technol. **21**, 1470 (1992).
 [2] T.C. Sangster, R.L. McCrory, V.N. Goncharov *et al.*, Nucl. Fusion **47**, S686 (2007).
 [3] J.F. Latkowski, A. Kubota, M.J. Caturla *et al.*, Fusion Sci. Technol. **43**, 540 (2003).
 [4] R.L. Bieri and M.W. Guinan, Fusion Technol. **19**, 673 (1991).
 [5] R.W. Moir, Fusion Eng. Des. **51-2**, 1121 (2000).
 [6] J.D. Sethian, M. Friedman, R.H. Lehmberg *et al.*, Nucl. Fusion **43**, 1693 (2003).
 [7] V.D. Zvorykin, S.V. Arlantsev, V.G. Bakaev *et al.*, *Inertial Fusion Sciences and Appl. 2003*, (B.A. Hammel, D.D. Meyerhoffer, J. Meyer-ter-Vehn and H. Azechi Eds., Amer-

- ican Nuclear Society, Inc., 2004) p.548.
- [8] C.D. Marshall, J.A. Speth and S.A. Payne, *J. Non-Cryst. Solids* **212**, 59 (1997).
- [9] J.F. Latkowski, A. Kubota, M.J. Caturla *et al.*, *Fusion Sci. Technol.* **43**, 540 (2003).
- [10] B.A. Levin, D.V. Orlinski, K.Yu. Vukulov *et al.*, *Problems of Atomic Science and Technology, Series: Physics of Radiation Effect and Radiation Materials Science, No.3*, p.51 (2003).
- [11] V.D. Zvorykin, N.V. Didenko, A.A. Ionin *et al.*, *Laser Part. Beams* **25**, 435 (2007).
- [12] S.P. Obenschain, J.D. Sethian and A.J. Schmitt, *Fusion Sci. Technol.* **56**, 594 (2009).
- [13] V.D. Zvorykin, S.V. Arlantsev, V.G. Bakaev *et al.*, *Laser Part. Beams* **17**, 609 (2001).
- [14] A.O. Levchenko, V.D. Zvorykin, S.V. Likhomanova *et al.*, *Quantum Electron.* **40**, 203 (2010).
- [15] P.B. Sergeev, A.P. Sergeev and V.D. Zvorykin, *Quantum Electron.* **37**, 706 (2007).
- [16] P.B. Sergeev, A.P. Sergeev and V.D. Zvorykin, *Quantum Electron.* **37**, 711 (2007).
- [17] A.P. Sergeev and P.B. Sergeev, *J. Opt. Technol.* **78**, 341 (2011).
- [18] A.S. Alimov, B.S. Ishkhanov *et al.*, *Moscow Univ. Phys. Bull.* **65**, 111 (2010).
- [19] V.D. Zvorykin, S.V. Arlantsev *et al.*, *J. Phys: Conference Series* **112**, 032055 (2008).